Global Optimization of Local Weights in Mixed-Cost MPC for Minimum Time Vehicle Maneuvering

Jeffery R. Anderson[1] and Beshah Ayalew[1]

Abstract— In this paper a Model Predictive Control (MPC) strategy is utilized to model a professional driver negotiating a set driving circuit in minimum time. MPC is inherently suboptimal because not all future information is incorporated into each horizon of the control scheme. Motivated by how professional drivers learn race circuits in order to best exploit its features, we will alleviate some of the suboptimality inherent to MPC by optimizing the local cost function of each MPC horizon. This will allows objectives over a local segment to be properly adjusted such that the global goal of minimizing maneuvering time over a full maneuver is approximated. This problem is solved utilizing a cascaded optimization structure with the inner loop recursively solving the MPC problem around the track and the outer loop optimizing the weights of the local MPC horizons. It will be shown that by varying weights at key locations on a particular maneuver, performance gains can be realized compared to a traditional time optimal MPC strategy.

I. INTRODUCTION

The study of minimum time maneuvering problems is a key problem in the automotive industry with many influences ranging from a direct impact to the motorsports industry [1] to other indirect influences on vehicle safety systems and high performance automobiles. A professional human driver is still regarded as the pinnacle of vehicular control when limit handling is concerned. A trained human driver has the ability to operate a vehicle in a highly nonlinear and unpredictable environment. Moreover, experience in testing and racing has shown different drivers can achieve nearly identical performance with different driving styles. We believe that by understanding how different drivers treat this control, ultimately these systems can be optimized for a specific style.

The main contribution of this paper is in modeling how a human treats vehicle control in this environment. For this, a cascaded optimization structure is used. In the inner loop, a mixed cost MPC is use to find the optimal driving controls (i.e., throttle, brake, and steering). In each local MPC segment, the controller blends the objectives of either minimizing maneuvering time or maximizing exit velocity over the local MPC segment. Next, the outer loop, acting on the full maneuver, identifies the optimal set of weights used in each local MPC segment such that the global maneuvering time is minimized.

This particular optimization structure was chosen based on insights from both literature and practical experience with

[1]Jeffery R. Anderson and Beshah Ayalew are with the Applied Dynamics & Control Group at the Clemson University - International Center for Automotive Research, 4 Research Drive, Greenville, SC 29607, USA, {jra3, beshah}@clemson.edu

professional drivers. First, MPC is utilized in the inner loop to mimic how a human drives. This choice is motivated by the work in [2] which makes the case that a human behaves more like a MPC than an optimal controller acting on the full maneuver. Next, the choice of minimizing time or maximizing exit velocity at each local segment can be motivated by the work in [3] which states that a driver exiting a curve will tend to favor one or the other objective based on track configuration. For example, it can be advantageous to global maneuvering time to maximize velocity at the exit of a turn that is followed by a long straight. In our previous work [4], we have shown how varying local MPC costs throughout a maneuver can have an advantage over the typical fixed-cost time optimal MPC. This work extends the previous study in two areas: a more detailed vehicle dynamics model and the capability to blend the two objectives within each horizon.

Solutions of minimum time vehicle maneuvering problems can be classified into three categories. Quasi-steady state methods find the best set of steady state conditions such that the maneuvering time is minimized [5], [6], [7]. Separated path planning and path following methods first optimize the racing line [8] and then track the resulting line in minimum time [9], [10], [11]. Finally, trajectory optimization directly utilizes optimal control theory to find the set of vehicle controls that minimize maneuvering time subject to path boundaries (road width constraints) and vehicle dynamic constraints [12], [13]. This last class of approaches will be utilized in this work.

Once the optimal control problem has been posed, one of two classes of solution methods are typically employed to solve the problem: direct methods and indirect methods. Indirect methods solve the optimal control problem by deriving the first order necessary conditions via application of Pontryagin's Minimum Principle and derivation of the adjoint system equations. The result of these conditions is a Hamiltonian boundary value problems which is typically solved numerically. The work found in [14], [15] are excellent examples that utilize this method. Direct methods, on the other hand, solve the problem by discretization of the system and casting the optimal control problem as a finite dimensional nonlinear programming problem (NLP). The work presented in [16], [17] are two good examples using this solution method. There is much discussion as to which solution technique yields better results including Sharp and Peng [18] which make the case for direct methods stating that they are more suited to the typical switching behavior in the optimal braking control found in these types of problems. Both methods have yielded excellent results

and there are many papers demonstrating solutions of either type. The work in [19], shows that the Lagrange multipliers used in direct methods are discrete approximations of the co-state variables found in the indirect methods. With either case, numerical techniques must be applied to solve either the NLP or two point boundary value problem. The full details of these methods are outside the scope of this paper; the reader is referred to [20], [21] for a thorough description.

As previously discussed, we will model the human element of driving via application of MPC and recursively solve the local optimal control problem at each MPC horizon. Originally, MPC was utilized as a means of overcoming numerical issues and was used to extend the optimal solution of a short segment to an arbitrarily long track [22]. There have been several other works that considered modeling the human element in driver control. The work in [23] attempts to address this problem with robust optimal control. The work in [24], [25] shows how boundary conditions and cost functions can be altered to reproduce advance driving techniques. Although not strictly motivated by minimum time maneuvering, [26] shows how varying cost functions can represent different driving styles. In this paper, we will build upon these works by locally optimizing each MPC horizon to effectively model the learning that a professional driver does on a new track.

This paper is organized as follows. First, a description of the vehicle model will be shown in Section II followed by a detailed description of our optimization framework in Section III. Next, results utilizing this solution technique will be presented in IV and finally, Section V will offer conclusions on this work.

II. VEHICLE MODEL

In this paper, a four wheel vehicle model that includes effects of load transfer, nonlinear tires, aerodynamics, and a differential is utilized. This model is heavily based on the literature found in [27], [17], [28]. For the purposes of this work, the following subscripts are used to denote wheel position. $(\cdot)_{\blacktriangleleft\blacktriangle}$, where: $\blacktriangleleft \in \{L, R\}$ is the left or right side and $\blacktriangle \in \{1, 2\}$ represents the front or rear axle, respectively. The vehicle sprung mass is modeled with three degrees of freedom for motion longitudinally (longitudinal velocity v_x), laterally (lateral velocity v_y), and rotation about the yaw axis (yaw rate $\dot{\psi}$).

$$\dot{v_x} = v_y \dot{\psi} + \frac{F_x}{m} \tag{1}$$

$$\dot{v_y} = -v_x \dot{\psi} + \frac{F_y}{m} \tag{2}$$

$$I_{zz}\ddot{\psi} = a(\cos(\delta)(F_{yR1} + F_{yL1}) + \sin(\delta)(F_{xR1} + F_{xL1})) + w_f(F_{yR1}\sin(\delta) - F_{xR1}\cos(\delta)) + w_f(F_{xL1}\cos(\delta) - F_{yL1}\sin(\delta)) + w_r F_{xL2} - b(F_{yR2} + F_{yL2}) - w_r F_{xR2} \tag{3}$$

where F_x and F_y denote the total lateral and longitudinal forces acting at the Center of Gravity (Cg):

$$F_x = \cos(\delta)(F_{xL1} + F_{xR1}) - \sin(\delta)(F_{yL1} + F_{yR1}) + F_{xL2} + F_{xR2} + F_{ax}$$
$$F_y = \cos(\delta)(F_{yL1} + F_{yR1}) + \sin(\delta)(F_{xL1} + F_{xR1}) + F_{yL2} + F_{yR2} \tag{4}$$

and the individual tire lateral and longitudinal forces are denoted by $F_{x\blacktriangleleft\blacktriangle}$ and $F_{y\blacktriangleleft\blacktriangle}$. Aerodynamic drag is denoted as F_{ax}.

In addition to the sprung mass, four differential equations are used to model the individual wheel dynamics.

$$\dot{\omega_{L1}} = \frac{(-T_{L1} + R_f F_{xL1})}{Jr_f} \tag{5}$$

$$\dot{\omega_{R1}} = \frac{(-T_{R1} + R_f F_{xR1})}{Jr_f} \tag{6}$$

$$\dot{\omega_{L2}} = \frac{(-T_{L2} + R_r F_{xL2})}{Jr_r} \tag{7}$$

$$\dot{\omega_{R2}} = \frac{(-T_{R2} + R_r F_{xR2})}{Jr_r} \tag{8}$$

The lateral and longitudinal dynamics are controlled through inputs: u_1, u_2 which are the steering rate and torque demand rate on the chassis. This allows for a convenient mechanism of placing state constraints to represent the human bandwidth of control and vehicle limitations. The steering angle and torque demand quantities are found by:

$$\dot{\delta} = u_1, \quad \dot{T} = u_2 \tag{9}$$

This paper assumes front steer only ($\delta_{L1} = \delta_{R1} = \delta$ and $\delta_{L2} = \delta_{R2} = 0$).

The torque allocation between the four wheels depends whether or not the vehicle is braking or accelerating. Under braking, the torque is distributed evenly left and right and via a distribution constant to the front or rear wheels ($kt_{braking}$). While driving, all of the vehicle torque is sent to the rear wheels; thus, $kt_{driving} = 1$. Because of this, the torque allocation (T) is separated into positive components: T^+, T^- in order to select the correct torque distribution to the rear wheels (k_t):

$$k_t = T^+ kt_{driving} + T^- kt_{braking} \tag{10}$$

Finally, the individual wheel torques are defined as:

$$\begin{array}{cc} T_{L1} = \frac{1-k_t}{2}T & T_{R1} = \frac{1-k_t}{2}T \\ T_{L2} = \frac{k_t}{2}T + k_d\Delta_\omega & T_{R2} = \frac{k_t}{2}T - k_d\Delta_\omega \end{array} \tag{11}$$

where k_d is the viscous differential constant and Δ_ω is difference in rear wheel speed; i.e., $\Delta_\omega = \omega_{L2} - \omega_{R2}$.

The aerodynamic model is used to capture the speed dependent down force and drag quantities acting on the vehicle. These forces are applied to the vehicle center of pressure (Cp) shown in Figure 1. The aerodynamic forces are described by:

$$F_{az} = \frac{1}{2}C_L \rho A v_x^2 \tag{12}$$

$$F_{ax} = \frac{1}{2}C_D \rho A v_x^2 \tag{13}$$

The constants C_L, and C_D are the downforce and drag coefficients respectively. The vehicle's frontal area is denoted as A and the air density is denoted as ρ. Other aerodynamic effects such as yaw and pitch coupling are neglected for the purposes of this work. The normal tire load is calculated
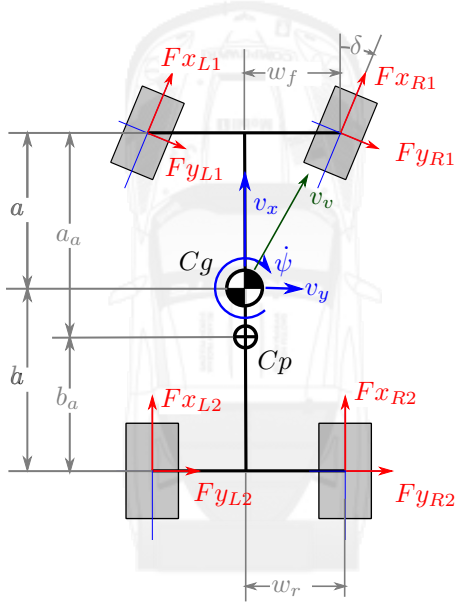

Fig. 1. Vehicle top view.

by summing forces and moments about the chassis and enforcing a roll stiffness distribution D between the front and rear axles:

$$\begin{bmatrix} 1 & 1 & 1 & 1 \\ -w_f & w_f & -w_r & w_r \\ -a & -a & b & b \\ D-1 & 1-D & D & -D \end{bmatrix} \begin{bmatrix} Fz_{L1} \\ Fz_{L2} \\ Fz_{L2} \\ Fz_{R2} \end{bmatrix} = \begin{bmatrix} -mg - F_{az} \\ -hF_y \\ (a_a - a)F_{az} + hF_x \\ 0 \end{bmatrix} \quad (14)$$

The tire friction forces are calculated via an empirical formula that is sensitive to changes in loads, lateral slip angle, and longitudinal slip. It is based on the simplified Pacejka tire model presented in [27], [17]. The slip ratio (κ) and slip angle (α) are calculated as:

$$\kappa = -\left(1 + \frac{R\omega}{v_{xtire}}\right) \quad (15)$$

and,

$$\alpha = -atan\left(\frac{v_{ytire}}{v_{xtire}}\right) \quad (16)$$

where R is the effective rolling radius of the tire and v_{xtire}, v_{ytire} are the longitudinal and lateral velocities of the tire at each wheel position accounting for rotation due to steering and chassis motion. As is common to this field, path intrinsic coordinates will be used to model the vehicle trajectory with respect to the road centerline. This

will facilitate a convenient mechanism for constraining the vehicle to stay within the track boundaries. As depicted in Figure 2, the heading deviation (e_ψ), lateral deviation (e_y), path referenced speed ($\dot{s}$) are as follows:

$$\dot{s} = \frac{v_x \cos(e_\psi) - v_y \sin(e_\psi)}{1 - e_y C} \quad (17)$$

where C is the path curvature and is assumed to be a known function of path distance i.e., $C = C(s)$.

$$\dot{e_\psi} = \dot{\psi} - C\dot{s} \quad (18)$$

$$\dot{e_y} = v_x \sin(e_\psi) + v_y \cos(e_\psi) \quad (19)$$

The full system description can be written as:

$$\dot{\mathbf{x}} = f(\mathbf{x}, \mathbf{u}, t) \quad (20)$$

where,

$$\mathbf{x} = \begin{bmatrix} e_\psi & e_y & v_x & v_y & \dot{\psi} & \omega_{\blacktriangleleft\blacktriangle} & \delta & T \end{bmatrix}^T \quad (21)$$

It is convenient to transform the system so that the final distance can be fixed . This transformation is conducted via application of the chain rule in (20):

$$\frac{d\mathbf{x}}{dt}\frac{dt}{ds} = \frac{d\mathbf{x}}{ds} = \frac{\dot{\mathbf{x}}}{\dot{s}} \quad (22)$$
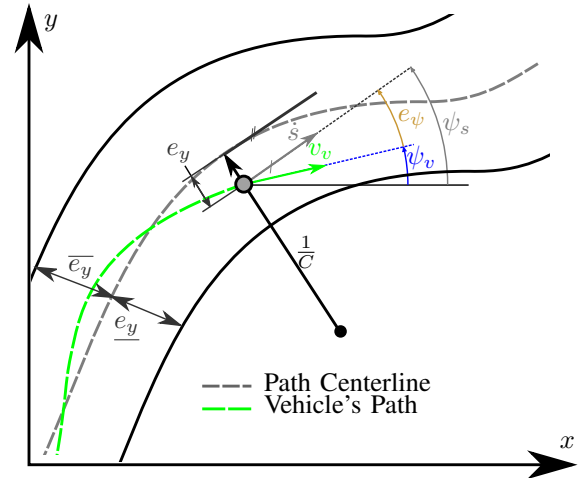

Fig. 2. Path intrinsic coordinate description. Note subscripts s and v refer to the path and vehicle frame respectively.

III. CASCADED OPTIMIZATION

The cascaded structure is comprised of a lower level controller which utilizes a variable cost MPC to drive the vehicle around the track while minimizing the cost function at each horizon. The variable cost allows the controller in a local horizon to blend two different objectives: minimizing time or maximizing exit velocity at the end of the horizon. The upper level optimization's objective is to find the optimal set of weights that the lower level controller will use in each local MPC horizon such that the global maneuvering time

$(t(s_{end}) - t(s_{start}))$ is minimized. The cascaded optimization can be written as:

$$
\begin{array}{|l|c|}
\hline
\min_{\mathbf{Z}} & J = t(s_{end}) - t(s_{start}) \\
\hline
& \begin{array}{|c|}
\hline
\text{Sub MPC Problem:} \quad for \; i = 1, 2, ..., N-1 \\
\hline
(25) \\
\hline
\begin{array}{c}
s^i \in \left[s_o^i \quad (s_o^i + s_{horizon}) \right] \\
s^{i+1} = s_o^i + \frac{(s_f - s_0)}{N} \\
x_0^{i+1} = x(s^{i+1})
\end{array} \\
\hline
\end{array} \\
s.t. \qquad\qquad w_k^i \in [0,1] \\
\hline
\end{array}
$$
(23)

where $\mathbf{Z}$, the decision variable of the outer loop, contains the set of weights (w_k^i, $k \in \{t, v_x\}$) used over each local MPC horizon. In other words:

$$
\begin{aligned}
\mathbf{Z} &= \left[\begin{array}{cccc} Z^1 & Z^2 & \dots & Z^{N-1} \end{array} \right]^T \\
&= \left[\begin{array}{cc|cc|c|cc} w_t^1 & w_{v_x}^1 & w_t^2 & w_{v_x}^2 & \dots & w_t^{N-1} & w_{v_x}^{N-1} \end{array} \right]^T
\end{aligned}
$$
(24)

Therefore, the global set of weights $\mathbf{Z} \in \mathbb{R}^{2(N-1) \times 1}$. Furthermore, each element of $\mathbf{Z}$ is such that $w_k^i \in [0,1]$. We use a genetic algorithm to find the globally optimal set of weights $\mathbf{Z}$. Supercomputing clusters were used to arrive at the results presented below.

The inner loop is responsible for solving the sub MPC problem over the prescribed maneuver while minimizing it cost function in each horizon given a weighting vector $\mathbf{Z}$.

Starting from the initial position (s_o) and with the initial states (x_0), an optimal control problem is posed over a finite preview horizon. For the purposes of this work, 150m was used a the preview horizon ($s_{horizon}$). Over this horizon, the optimal control problem can be written as:

$$
\begin{aligned}
\min_{u} \quad & J(x, x(s), u(s), w_k) = (26) \\
s.t. \quad & \frac{d\mathbf{x}}{ds} - f(s, x(s), u(s)) = 0 \\
& h(s, x(s), u(s)) \leq 0 \\
& g_b(x(s_0), x(s_f), u(s_o), u(s_f)) = 0
\end{aligned}
$$
(25)

where J is a general cost-functional that will be further clarified in the proceeding discussion. The function $f(\cdot) \in \mathbb{R}^n$ represents the system dynamics described by (22). The function $g(\cdot) \in \mathbb{R}^{n_g}$ is used to constrain the lateral deviation of the vehicle to stay within the track width boundaries ($\underline{e_y} \leq e_y \leq \overline{e_y}$) and to limit the maximum engine power ($\overline{P_{eng}} = T\omega_{rear} \leq P_{eng}^{max}$). The function $g_b(\cdot) \in \mathbb{R}^{n_{gb}}$ captures boundary conditions of the problem. Once the first local optimal control problem is solved, the preview horizon is then shifted by the MPC update interval ($(s_f - s_0)/N$) and the initial conditions are updated for the next horizon. For the purposes of this work, a 10m MPC update interval was utilized. The optimal control is computed over the new horizon and the process is repeated around the entire track for each $i = 1, 2, ..., N-1$ MPC horizons.

Each local optimal control problem was solved via an orthogonal collocation method with an adaptive mesh refinement implemented in the GPOPS-II software package [29].

In the cascaded optimization formulation, a mixed cost function capable of blending the objectives of minimizing

the local segment maneuvering time and exit velocity will be used. The two objectives are balanced via the weighting terms w_k. Where the subscript $k \in \{t, v_x\}$ denotes either time or longitudinal velocity.

$$
J_{MPC}^i(Z^i) = \underbrace{w_t^i \left(\frac{t(s_{horizon}^i)}{s_t} \right)^2}_{\text{Minimize Time}} - \underbrace{w_{v_x}^i \left(\frac{v_x(s_{horizon}^i)}{s_{v_x}} \right)^2}_{\text{Maximize Exit Velocity}}
$$
(26)

In this cost structure, proper scaling between the objectives is handled via the scaling terms, s_t and s_{v_x} which are fixed throughout the maneuver and are the maximum values of velocity and time over each horizon found in the reference time optimal MPC case discussed next.

To facilitate comparison, a time optimal MPC will be used. The time optimal cost function for each horizon can be written as:

$$
J_t^i = \int_{s_0^i}^{s_{horizon}^i} \frac{1}{\dot{s}} ds
$$
(27)

IV. RESULTS AND DISCUSSION

In this section, the preceding optimizations were carried out. For comparison, the globally optimized MPC will be compared to the traditional, fixed-cost, time optimal MPC. The maneuver used in this simulation is a chicane segment of a racing circuit. The vehicle model parameters used in this study were identical to those published in [17]. A comparison of trajectories can be seen in Figure 3. Note to simulate the "out lap" and "in lap" that a human driver takes before and after a typical timed maneuver, the metric maneuvering time is calculated as $t(s_{end}) - t(s_{start})$ were $s_{start} = 0m$ and $s_{end} = 650m$; however, the simulation solved the domain $s \in [-50m \; 750m]$. For the trajectories in a macro view, the racing lines are extremely similar; however, looking at the difference in lateral deviation between the two solutions versus distance around the track (Figure 4) shows that they are indeed quite different with almost 0.7m deviation occurring just after point ②. This can be considered a substantially different racing line through this section of the maneuver. The values of the weights themselves w around the track are quite noisy as seen in Figure 5; however, conclusions can still be drawn. If the contribution of the velocity weight, i.e., $w_{v_x}/(w_t + w_{v_x})$ is plotted along side the track curvature. Distinct spikes in w_{v_x} contributions can be seen when the curvature is changing (Figure 6). On the straight portions of track, the two objectives minimizing time and maximizing velocity are nearly identical objectives (albeit some subtleties exist) and contribute to the noise seen in these weights; thus, the reason for the highlights in the plot. The difference in these solutions manifest themselves mainly at two key points over the maneuver seen in Figure 7 (approximately ① = 125m and ② = 240m). These two points demonstrate exactly what the algorithm is capable of doing. The outer loop sees a section of track where it is beneficial to sacrifice some speed at the local section of track ① to maintain a higher velocity later in the maneuver ② where it is more
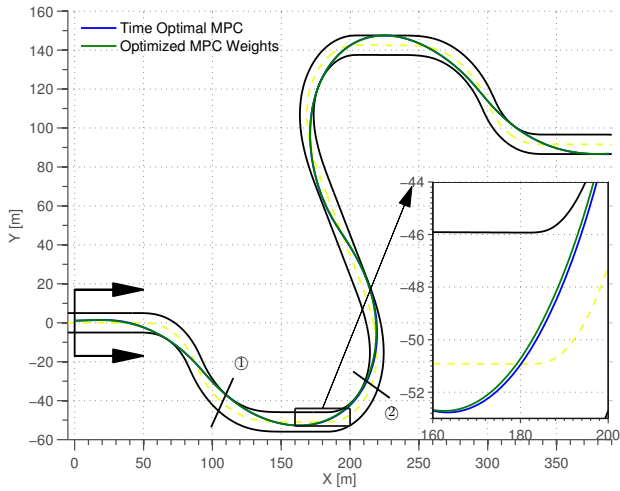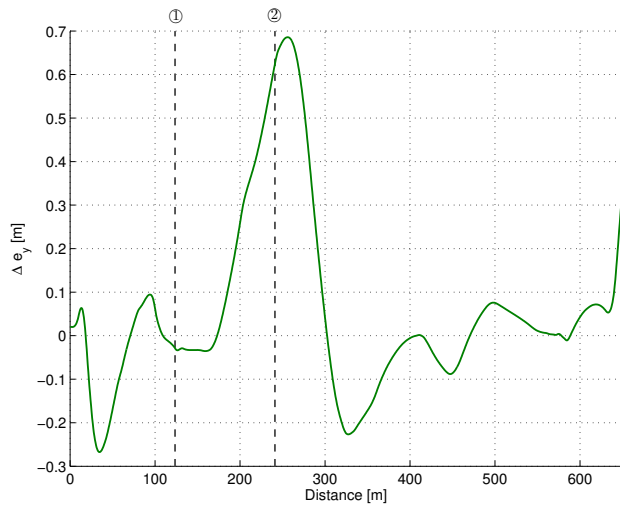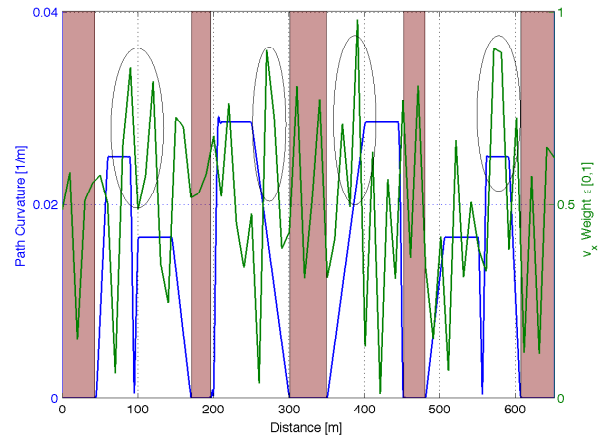
Fig. 3. Vehicle trajectories.

Fig. 6. Contribution of weight of exit velocity $w_{v_x}/(w_t + w_{v_x})$ and track curvature. Note the circled spikes in section of the track where the curvature is changing. The highlighted region denotes a straight path segment.

TABLE I

RESULTS FROM SIMULATION APPROACHES.

Simulation	Time [s]	Difference [%]
Time Optimal MPC	14.493	0.00%
Optimized Cost MPC	14.446	-0.33%

important to the global objective. In other words, some speed is sacrificed in the high speed section of the track to maintain higher speed through the low speed section of the track yielding a net improvement in performance over the entire maneuver. Figure 8 show a comparison of the vehicle steering and throttle differences in the two control strategies and Table I show the final maneuvering times and performance differences. In spite of the difference in

Fig. 4. Difference in racing line versus track distance of the two solutions.
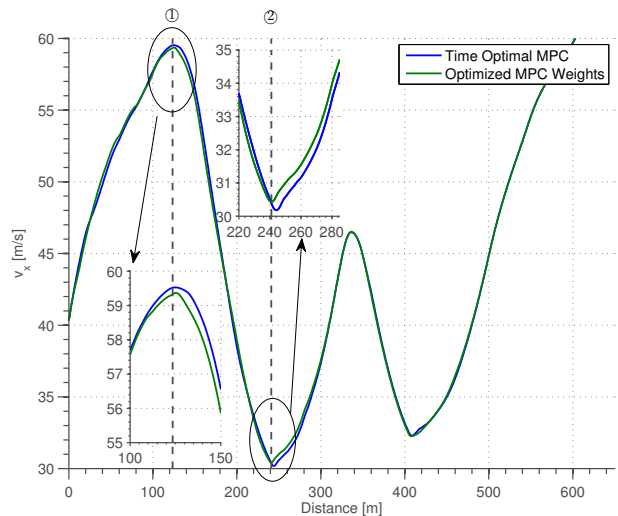Note: $\Delta e_y = e_y(s)|_{timeOpt} - e_y(s)|_{locallyOptMpc}$.

Fig. 7. Velocity comparison.

maneuvering times being relatively small, a very different driving strategy is used to find these small gains. Moreover, in the context of motorsports and vehicle minimum time maneuvering problems, millisecond differences in performance separate top teams in key races such as Formula 1 and Le
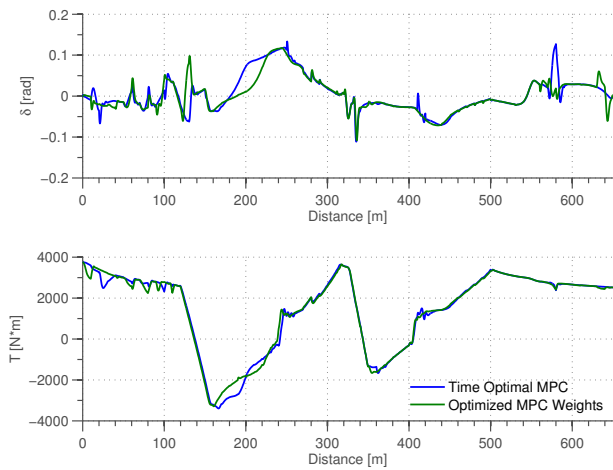

Fig. 5. Optimized weights $\mathbf{W}$ around the chicane maneuver.

Fig. 8.   Steering and throttle demand.

Mans. In the top tiers of motorsports, millions of dollars are spent for milisecond gains [21], [30].

V. CONCLUSIONS

In this paper, we model a human driver controlling a vehicle to negotiate a set maneuver in minimum time using MPC. Future path preview information is incorporated into the local MPC problem by extending the local horizon cost function to include two terms in order to blend the objectives, minimization of time over the horizon and maximization of the exit velocity for the horizon. The weights of these two terms were then optimized for each MPC segment over the entire maneuver in order to globally minimize maneuvering time. This framework was then applied to a chicane maneuver and yielded performance benefits over the traditional time optimal MPC controller. Moreover, these seemingly slight gains were accomplished via very different control histories. As previously mentioned, human drivers can achieve very similar performances with drastically different driving styles.

REFERENCES

[1] P. Wright and T. Matthews, "Formula 1 technology," SAE Technical Paper, Tech. Rep., 2001.

[2] D. Casanova, "On minimum time vehicle manoeuvering: The theoretical optimal lap," Ph.D. dissertation, Cranfield University, November 2000.

[3] M. Maniowski, "Optimisation of driver actions in rwd race car including tyre thermodynamics," *Vehicle System Dynamics*, vol. 54, no. 4, pp. 526–544, 2016.

[4] J. R. Anderson, B. Ayalew, and T. Weiskircher, "Modeling a professional driver in ultra-high performance maneuvers with a hybrid cost MPC," in *American Control Conference (ACC), 2016*.   IEEE, July 2016, pp. 1981–1986.

[5] D. Brayshaw and M. Harrison, "A quasi steady state approach to race car lap simulation in order to understand the effects of racing line and centre of gravity location," *Proceedings of the Institution of Mechanical Engineers, Part D: Journal of Automobile Engineering*, vol. 219, no. 6, pp. 725–739, 2005.

[6] A. Tremlett, F. Assadian, D. Purdy, N. Vaughan, A. Moore, and M. Halley, "Quasi-steady-state linearisation of the racing vehicle acceleration envelope: a limited slip differential example," *Vehicle System Dynamics*, vol. 52, no. 11, pp. 1416–1442, 2014.

[7] W. F. Milliken and D. L. Milliken, *Race Car Vehicle Dynamics*. SAE International, 1995.

[8] L. Cardamone, D. Loiacono, P. L. Lanzi, and A. P. Bardelli, "Searching for the optimal racing line using genetic algorithms," in *Conference on Computational Intelligence and Games*.   IEEE, August 2010, pp. 388–394.

[9] R. Sharp, D. Casanova, and P. Symonds, "A mathematical model for driver steering control, with design, tuning and performance results," *Vehicle System Dynamics: International Journal of Vehicle Mechanics and Mobility*, vol. 33, no. 5, pp. 289–326, 2000.

[10] T. Lipp and S. Boyd, "Minimum-time speed optimization over a fixed path," *International Journal of Control*, vol. 1, no. 1, pp. 1–15, 2014.

[11] P. A. Theodosis and J. C. Gerdes, "Generating a racing line for an autonomous racecar using professional driving techniques," in *ASME 2011 Dynamic Systems and Control Conference*, 2011, pp. 853–850.

[12] V. Cossalter, M. Da Lio, R. Lot, and L. Fabbri, "A general method for the evaluation of vehicle manoeuvrability with special emphasis on motorcycles," *Vehicle system dynamics*, vol. 31, no. 2, pp. 113–135, 1999.

[13] D. Casanova and R. Sharp, "Minimum time manoeuvring: The significance of yaw inertia," *Vehicle System Dynamics*, vol. 34, no. 34, pp. 77–115, 2000.

[14] J. Hendrikx, J. Meijlink, and R. Kriens, "Application of optimal control theory to inverse simulation of car handling," *Vehicle System Dynamics*, vol. 26, pp. 449–461, 1996.

[15] E. Bertolazzi, F. Biral, and M. Da Lio, "Symbolic–numeric indirect method for solving optimal control problems for large multibody systems," *Multibody System Dynamics*, vol. 13, no. 2, pp. 233–252, 2005.

[16] J. Allen, "Computer optimization of cornering line," Master's thesis, Cranfield University, 1997.

[17] G. Perantoni and D. J. Limebeer, "Optimal control for a formula one car with variable parameters," *Vehicle System Dynamics*, vol. 52, no. 5, pp. 653–678, 2014.

[18] R. Sharp and H. Peng, "Vehicle dynamics applications of optimal control theory," *Vehicle System Dynamics*, vol. 49, no. 7, pp. 1073–1111, July 2011.

[19] D. Garg, M. Patterson, W. W. Hager, A. V. Rao, D. A. Benson, and G. T. Huntington, "A unified framework for the numerical solution of optimal control problems using pseudospectral methods," *Automatica*, vol. 46, no. 11, pp. 1843–1851, 2010.

[20] J. T. Betts, "Survey of numerical methods for trajectory optimization," *Journal of guidance, control, and dynamics*, vol. 21, no. 2, pp. 193–207, 1998.

[21] D. J. Limebeer and A. V. Rao, "Faster, higher and greener: Vehicular optimal control," *IEEE Control Systems Magazine*, pp. 37–56, April 2015.

[22] D. Kelly and R. Sharp, "Time-optimal control of the race car: a numerical method to emulate the ideal driver," *Vehicle System Dynamics*, vol. 48, no. 12, pp. 1461–1474, 2010.

[23] J. Timings and D. Cole, "Robust lap-time simulation," *Proceedings of the Institution of Mechanical Engineers, Part D: Journal of Automobile Engineering*, vol. 228, no. 10, pp. 1200–1216, 2014.

[24] E. Velenis and P. Tsiotras, "Minimum time vs maximum exit velocity path optimization during," *IEEE*, pp. 355–360, June 2005.

[25] E. Velenis, P. Tsiotras, and J. Lu, "Optimality properties and driver input parameterization for trail-braking cornering," *European Journal of Control*, vol. 4, pp. 308–320, 2008.

[26] G. Prokop, "Modeling human vehicle driving by model predictive online optimization," *Vehicle System Dynamics*, vol. 35, no. 1, pp. 19–53, 2001.

[27] D. Kelly, "Lap time simulation with transient vehicle and tyre dynamics," Ph.D. dissertation, Cranfield University, May 2008.

[28] A. Tremlett, M. Massaro, D. Purdy, E. Velenis, F. Assadian, A. Moore, and M. Halley, "Optimal control of motorsport differentials," *Vehicle System Dynamics*, vol. 53, no. 12, pp. 1771–1794, 2015.

[29] M. A. Patterson and A. V. Rao, "GPOPS-II: A matlab software for solving multiple-phase optimal control problems using hp-adaptive gaussian quadrature collocation methods and sparse nonlinear programming," *ACM Transactions on Mathematical Software*, vol. 41, no. 1, pp. 1–37, October 2014.

[30] A. Trabesinger, "Formula 1 racing: Power games," *Nature*, vol. 447, no. 7147, pp. 900–903, June 2007.